INTERNATIONAL JOURNAL OF AUTOMOTIVE AND MECHANICAL ENGINEERING (IJAME)
ISSN: 2229-8649 e-ISSN: 2180-1606
VOL. 19, ISSUE 3, 10014 – 10027
DOI: https://doi.org/10.15282/ijame.19.3.2022.13.0773

ORIGINAL ARTICLE

Dynamic Fatigue Behavior of Hip Joint under Patient Specific Loadings

T. Joshi[1,*], R. Sharma[1], V. Mittal[2], V. Gupta[3] and G. Krishan[4]

[1]Department of Mechanical Engineering, Amity University Haryana, 122413, India
[2]Department of Mechanical Engineering, NIT Kurukshetra, 136119, India
[3]Department of Mechanical Engineering, CDLSIET Panniwala Mota, 125077, India
[4]School of Innovation, Design and Technology, Wellington Institute of Technology, Wellington, New Zealand

ABSTRACT – In the present work, a finite element model with standard Charnley's implant of hip joint is considered for investigation under different patient-specific dynamic activities obtained in vivo. The application of forces occurred due to human movement, which ultimately generates dynamic stress over the prosthesis. Anatomical loading constraints are more clinically relevant than ISO standards. The performance of different materials for each suitable gait pattern is analyzed using commercial finite element code. A liner isotropic material Ti-6Al-4V and PMMA material is utilized for an implant and bone cement, respectively. However, cortical and cancellous bone are treated as non-isotropic in nature. Clinically obtained dynamic forces and torque are being used for the present investigation. Additionally, Goodman, Solderberg, Gerber and ASME elliptic fatigue theories were considered to obtain the fatigue life of the implant. The most strenuous activity in terms of stress and strain are, going downstairs followed by going upstairs, walking, standing up and sitting down, which have been found in good agreement with the safety factor for every activity. Additionally, the life expectancy of the implant was a minimum of 23 years under every dynamic motion. The present work exhibits the greater relevance in terms of the life expectancy of implant for the pre-surgical analysis before implanted in vivo.

ARTICLE HISTORY
Received: 3rd Mar 2022
Revised: 21st Sept 2022
Accepted: 20th Oct 222
Published: 28th Oct 2022

KEYWORDS
Gait cycle;
Fatigue life;
Dynamic loading;
Abductor muscle;
Charnley

INTRODUCTION

The hip joint is an important weight-bearing and shock-absorbing ball and socket joint in the human body. Additionally, it plays a very significant role in the movement like normal gait, running, climbing and jumping. Hip replacements have been performed to reduce pain induced by disease and injuries. Hip arthroplasty/replacements are successfully applied to patients undergoing diseases [1–4]. Hip arthroplasty was introduced in 1938, and extensively (0.3 million) surgeries are being performed worldwide every year [5]. The study of hip prostheses is interesting due to the reduction of minimum repeated surgical revision, especially in younger patients [5–7]. Forces applied by human activity to the hip prosthesis generate dynamic stresses varying with time and lead to dynamic failure of the implant. Consequently, it is significant to ensure implant resistance against dynamic failure. Fatigue and dynamic failure have significantly reduced in the last three to four decades due to material and design advancements [8,9]. More than two million Total Hip Replacements (THR) are being performed annually worldwide. The number of surgeries has increased rapidly in recent times due to an increase in the aged population [10]. As per the Canadian Joint Replacement Surgery report (2018-2019), the number of THR has increased by 20.1% in the last five years [11]. For instance, in the last ten years, 26% and 22% of revision surgeries have been reported in Sweden [12] and US, respectively [13]. Every new implant design and material has to be insured against fatigue failure. The success of an implant largely depends upon its compatibility and attachment to the bone cement and ultimately, to the host bone. Failure and loosening between cement-metal and cement-bone interfaces initiate the fracture and which may lead to revision surgeries [14]. Implant showcase higher stress at the interface fixation area, which may lead to a short or long-term failure occurs under dynamic gait movement [15,16].

Most of the stems for hip arthroplasty are made up of titanium alloys. Ti-6Al-4V alloys are extensively used as a biomaterial due to their excellent biocompatibility, high mechanical strength, chemical inertness, and modulus, which is half of the cobalt-chromium alloys [17,18]. The modulus of a metallic prosthesis (E= 110-220 GPa) is much higher than the host bone (E=15-20 GPa). High stiffness leads to stress shielding around the femoral prosthesis [19]. The higher modulus of implant leads to modulus mismatch, that's why an interface layer of bone cement is used between the implant (E=110 GPa) and bone (E=18 GPa). However, a very low stiffness leads to small migration of prosthesis and subsequent micro dislocations [20]. Multiple materials from high to low modulus with different combinations are being tested to observe and reduce the stress shielding effect and increase anatomical mobility [21,22]. Some of the investigations suggest that shape optimization with geometric remodeling is an alternative approach to reduce stress shielding and bone resorption [23–25]. An implant should fulfills the structural and mechanical demands of the hip joint. El 'Sheikh et al. [26] used the finite element technique to optimize design as well as material for artificial hip joints under peak static load

*CORRESPONDING AUTHOR | T. Joshi | ✉ tanujjoshi15@gmail.com

and stumbling dynamic loading conditions. Peak von mises stress and stress volume are to be measured in the study. It is concluded that stress volume is preferred for precise analysis of hip joints.

In the present work, a femoral prosthesis with bone cement and inserted Charnley's implant were tested under dynamic analysis with patient-generated gait data. Activities like walking, going up-down stairs, standing up and sitting down have been considered for present work. For the analysis, a three-dimensional model of a human femur, bone cement and implant have been constructed as per the bone geometries. Anatomical forces generated by the human body, retracting abductor muscle forces and induced torsional moment acting over the prosthesis are major considerable forces and moments which have been considered for the present study. The main aim of this study is to evaluate the performance of combination under different dynamic loading conditions and to check the implant life, which leads to the development of better implant design with extended life. Essential mechanical properties like stress, strain and deformation have been analyzed using the FEM technique and compared with other dynamic activities.

MATERIAL AND METHOD

Finite Element Modeling

The FEM technique [27–30] is a fast and efficient technique widely employed for solving complex shape analysis. Additionally, these techniques are used to assist and optimize the design of hip prostheses and provide an understanding of their mechanical behavior under multiple loading constraints [31–33]. The finite element model of the prosthesis assembly is depicted in Figure 1. A three-dimensional model of the hip joint was created using standard Charnley's implant. The modeling of the cortical and cancellous segments of the bone was done separately using SolidWorks to develop a suitable shape similar to actual human bone. All the components i.e., metallic implant, bone cement, cortical and cancellous, were assembled and repositioned to mimic the anatomical posture of the human body [34–36].

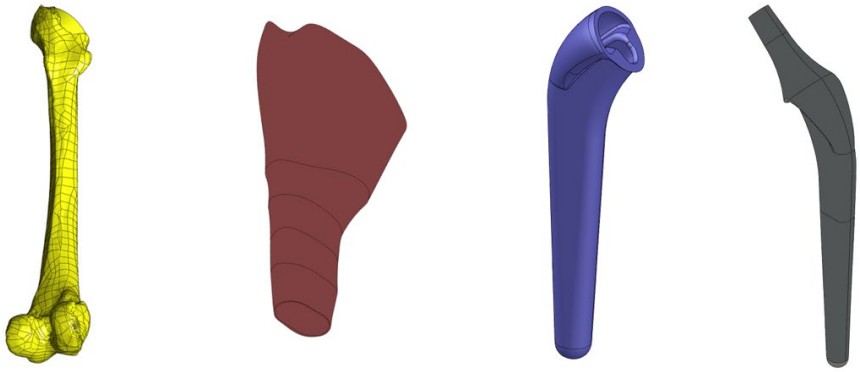

(a) (b) (c) (d)

Figure 1. Hip joint assembly, (a) cortical bone, (b) cancellous bone, (c) cone cement, (d) implant.

Materials

Titanium alloys are said to be the most suitable implant material in terms of biocompatibility, corrosion resistivity and mechanical strength [17]. Materials for both implant and bone cement are linear isotropic, but not in the case of bone. The inner and outer side of the bone (cancellous and cortical) is modeled with a transversely isotropic material combination. Assembly components with their essential mechanical properties are tabulated in Table 1 and 2.

Table 1. Material properties of hip stem and bone cement materials [31, 37, 38].

Materials	Density (kg/m^3)	Modulus (GPa)	Poission's ratio	Ultimate strength (MPa)	Yield strength (MPa)
Ti-6Al-4V	4500	110	0.32	900	800
PMMA	1200	2.64	0.4	-	43.8

Table 2. Material properties of cortical and cancellous bone [39].

Materials	Density (kg/m^3)	Modulus (GPa)	Shear modulus (GPa)	Poisson's ratio
Cortical bone	600	Ex = 11.5 Ey = 11.5 Ez = 17	Gxy = 3.6 Gxy = 3.3 Gxy = 3.3	υxy = 0.51 υxy = 0.51 υxy = 0.31
Cancellous bone	1900	E = 2.7	-	υ = 0.35

Meshing and Boundary Condition

The structural element of ten-node tetrahedral elements are considered for generating mesh. Tetrahedral elements have three degrees of freedom (DOF) at each node (translation into x, y and z-direction) and a quadratic displacement behavior well suited for irregular and complex bodies. The total number of nodes and elements for bone assembly were 652753 and 353197, respectively see Figure 3. Increasing the element number represents the real-world body more accurately. The meshed model of femur assembly is shown in Figure 2.

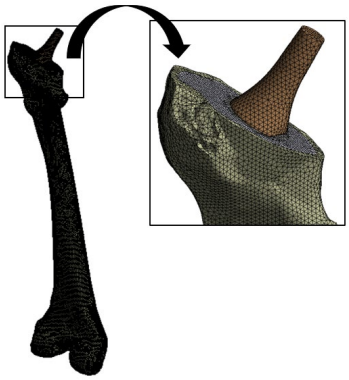

Figure 2. Meshed model of femur bone.

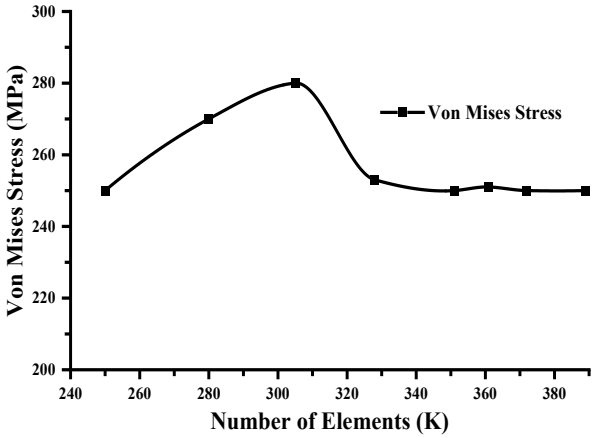

Figure 3. Mesh independency test.

Figure 4 describes the boundary conditions i.e., forces and support constraints. Time-dependent patient-specific dynamic forces and torque are extracted from Bregmann et al. [40]. A major retracting force of the abductor's muscle ($F_{abductor}$) is applied to the proximal region of the greater trochanter. Furthermore, a distal (lower) end of the femur remains to fix and does not allow it to move horizontally and vertically [41].

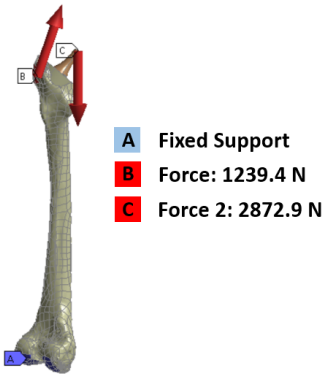

Figure 4. Boundary and loading constraints.

Validation with Prior Studies

No other studies examined mechanical characteristics with implant material for such a wide range of dynamic activities and compared them with previous studies. A prior study of implant assembly used approximately similar design configurations. Şensoy et al. [41] exploit the CT scan data to create a finite element model of a hip prosthesis with ten biocompatible materials. Dynamic peak joint forces and abductor muscle forces were applied over the prosthesis. It was concluded that austenitic, annealed, and bio-durable stainless steel is the best-suited material in terms of micromotions with 20.69% less strain value compared to Ti-6Al-4V assembly. In our present model with Şensoy et al. [41], loading constraints showed almost similar results. The comparison of deformation between Şensoy et al. and the present model with percentage deviation are tabulated in Table 3.

Table 3. Validation of present work deformation (mm) with Şensoy et al. [41].

Materials	Implant	Bone cement	Cancellous bone	Cortical bone
Present work	14.941	13.163	14.067	14.253
Şensoy et. al.	16.59	13.99	14.75	14.94
Percentage error (%)	9.93	5.91	4.63	4.59

RESULTS

Preliminary static and dynamic studies have been carried out to investigate the mechanical behavior of hip arthroplasty with standard Charnley's implant manufactured with Ti-6Al-4V material and Poly (methyl methacrylate) PMMA bone cement. It was noticed that the resultant mechanical parameter changes significantly with every dynamic activity and becomes constant with the static analysis.

Static Analysis

Von Mises stress

The load applied over any of the structural body causes stress generation. In the present work, the static human anatomical loadings (caused by human weight) are applied over the hip implant at a standing position. Stress generation in the hip joint is depicted in Figure 5. It can be seen that maximum stress has developed over the femoral implant, which can be seen in Figure 5(b). This occurs because the implant (after hip surgery) is the main structural part that bears the upper body loadings and transfers it towards the femur bone. Furthermore, the stress reduces accordingly towards cancellous bone (in Figure 5(e)), cortical bone (in Figure 5(d)), and bone cement (in Figure 5(c)). The maximum stress on an implant is being developed at the proximal end. However, for cortical and cancellous bone, it is maximum at the proximal end and medial side. Similar results are demonstrated by Sensoy et al. [41] for approx similar prosthesis configurations.

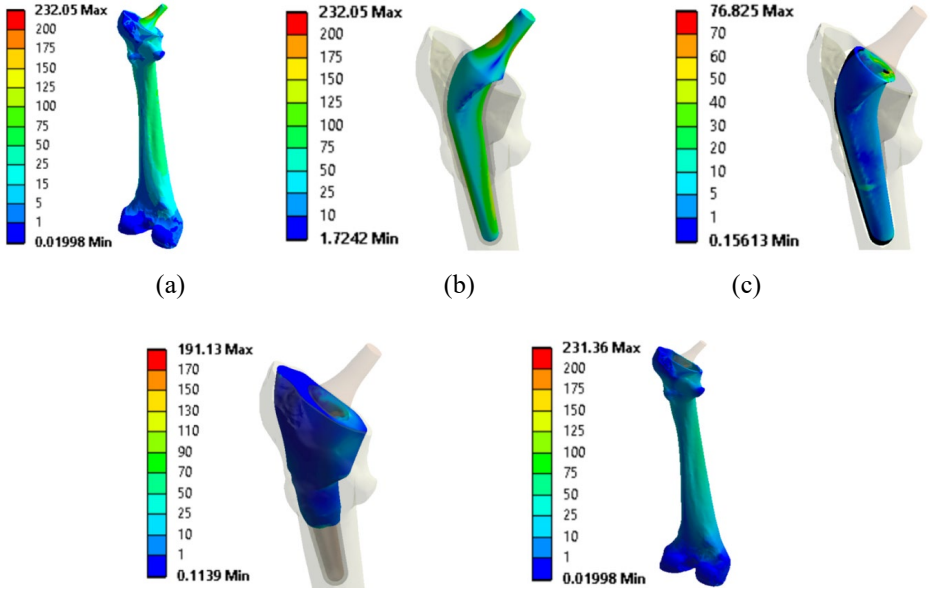

Figure 5. Von Mises stress for (a) bone assembly, (b) cortical bone, (c) implant, (d) bone cement and (e) cancellous bone.

Deformation

The deformation contours for static (standing) analysis for hip joint assembly are depicted in Figure 6(a) to 6(e). The implant has demonstrated maximum deformation at the proximal end. This could be due to the maximal load (body weight) applied at the proximal end. A similar trend in static analysis is followed by Sensoy et al. [41]. Maximum deformation has been developed over the implant (see Figure 6(b)), followed by cancellous bone (can be seen in Figure 6(e)), cortical bone (Figure 6(d)) and bone cement (see Figure 6(c)). The maximum deformation has been generated at the proximal side of every hip joint member, i.e., implant, bone cement, cancellous bone, and cortical bone and continuously reduces toward the distal end.

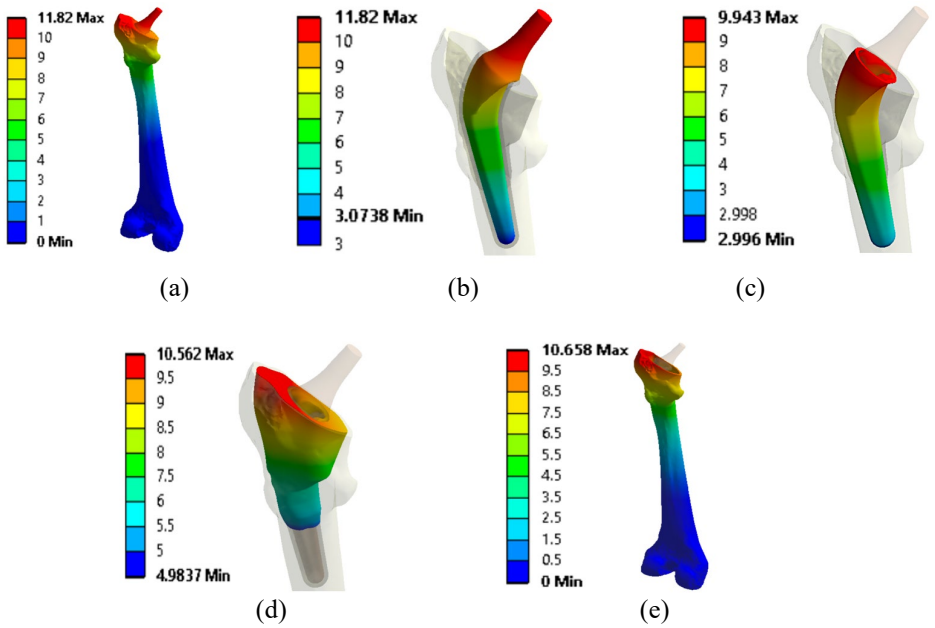

Figure 6. Deformation for walking at various percentages of the gait cycle; (a) bone assembly, (b) cortical bone, (c) implant, (d) bone cement, and (e) cancellous bone.

Strain

Strain is largely correlated with stress and depends upon the modulus of the parts. The strain contours for hip joint assembly are demonstrated in Figures 7(a) to 7(e). Similar to stress, maximum strain is demonstrated by cancellous bone (in Figure 7(d)) followed by bone cement (in Figure 7(b)), cortical bone (in Figure 7(e)) and implant (Figure 7(b)). The concentration of strain is localized at the interior side of the proximal end. Low modulus parts of the hip joint assembly like cancellous and cortical bone demonstrates higher strain value as compared to stiff parts.

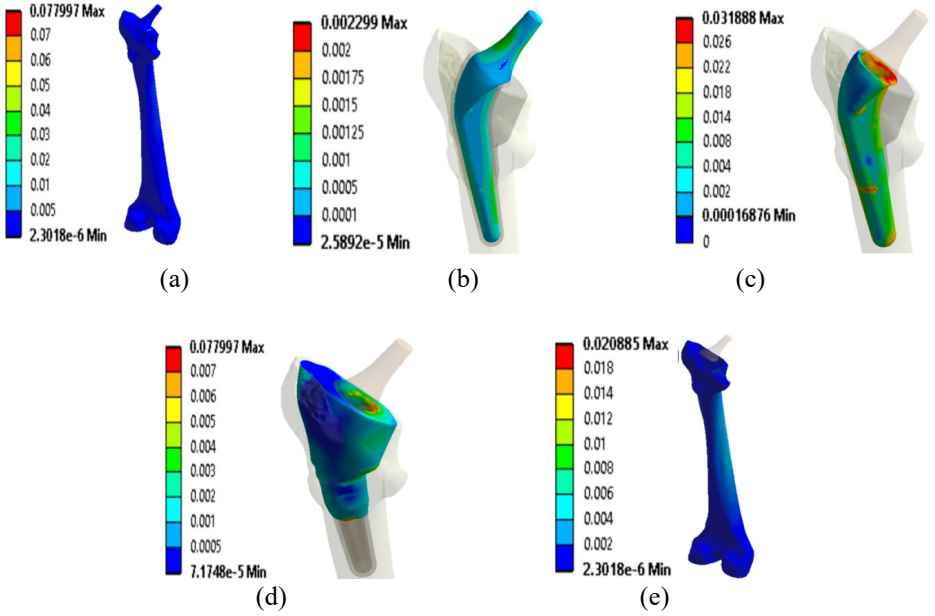

Figure 7. Strain for walking at various percentages of the gait cycle; (a) bone assembly, (b) implant, (c) bone cement, (d) cancellous bone and (e) cortical bone.

Dynamic Analysis

Static analysis is important in terms of mechanical acceptance, stability of the human joint, and standing position. However, the performance of hip joint does not only rely on static analysis method. The main functionality of hip joint is only demonstrated by its performance during the human gait cycle. The present section demonstrates mechanical parameters like stress, strain and deformation during human gait movements like walking, going down stairs, going up stairs, standing up and sitting down. In addition, contours of dynamic walking motion and variation into stress, strain and deformation were depicted in mainly four instances, i.e., 25, 50, 75, and 100% of the gait cycle.

Von Mises stress

Stress is the result of the loadings; as loading changes, the values of stress also change. The contour of stress for walking gait with bone assembly has been illustrated in Figure 8. Stress on implant assembly, cortical bone, implant, bone cement and cancellous bone are shown in Figure 8(a) to 8(e), respectively. Stress is maximum at the proximal end of the implant, medial side of bone cement and cancellous bone (see Figure 8). Whenever the heel of the human lands on the ground, a maximum amount of force is generated over the bone (15-20% of gait) and continuously reduces towards the mid-stance phase, i.e., the foot landed completely (32-98 % gait). In order to walk again, a person lifts their foot from the mid-stance phase (45 % gait) for the next step. At the same instance, the Toe-off condition of the gait occurs and leads to an increase in the forces over the bone (peak force at 50% of gait). Thereafter, the stress drastically reduces to its minimum level at the swinging phase (75-95 % gait). The same process is repeated over time. The maximum stress occurs at the heel strike phase then, reduces at the mid instance, increases to the toe off and then drastically reduces to a minimum at the swinging phase.

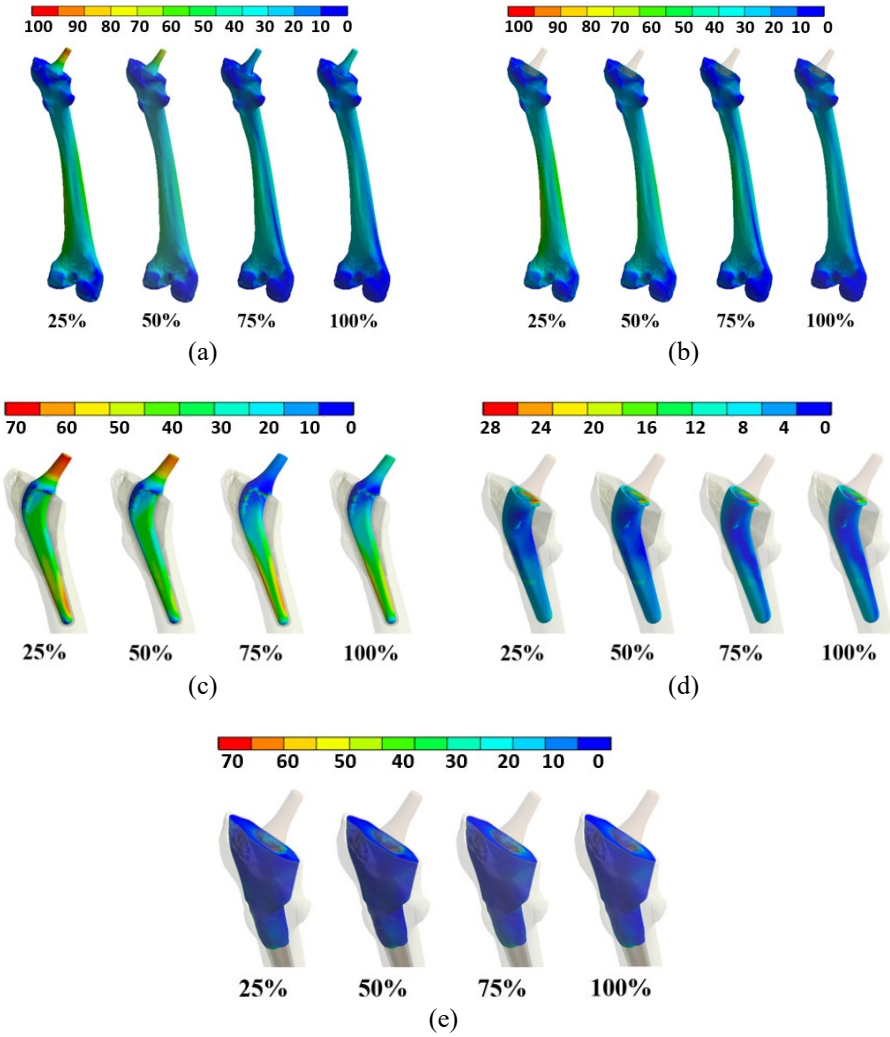

Figure 8. Von Mises stress for walking at various percentages of the gait cycle; (a) bone assembly, (b) cortical bone, (c) implant, (d) bone cement and (e) cancellous bone.

The next step of investigation involves different patient-specific dynamic gait movements, i.e., walking, going upstairs, going downstairs, standing up and sitting down with the same implant model. The stress variation for previously mentioned gait cycles has been presented in Figure 9 (a) to 9(e), respectively. Figure 9(a) demonstrates the stress perceived by all bone assembly parts, i.e., implant, bone cement, cancellous and cortical bone. At the peak forces, the maximum stress occurs at the implant, followed by cortical bone, cancellous bone and lastly by bone cement (see Figure 9(a) to 9(c). In standing up and sitting down movements, the foot does not undergo motions like stance and swing; that's why lesser peak forces are generated as compared to other motions. For every gait motion, cortical bone demonstrates higher forces than cancellous, and bone cement always showcases the least value of stress.

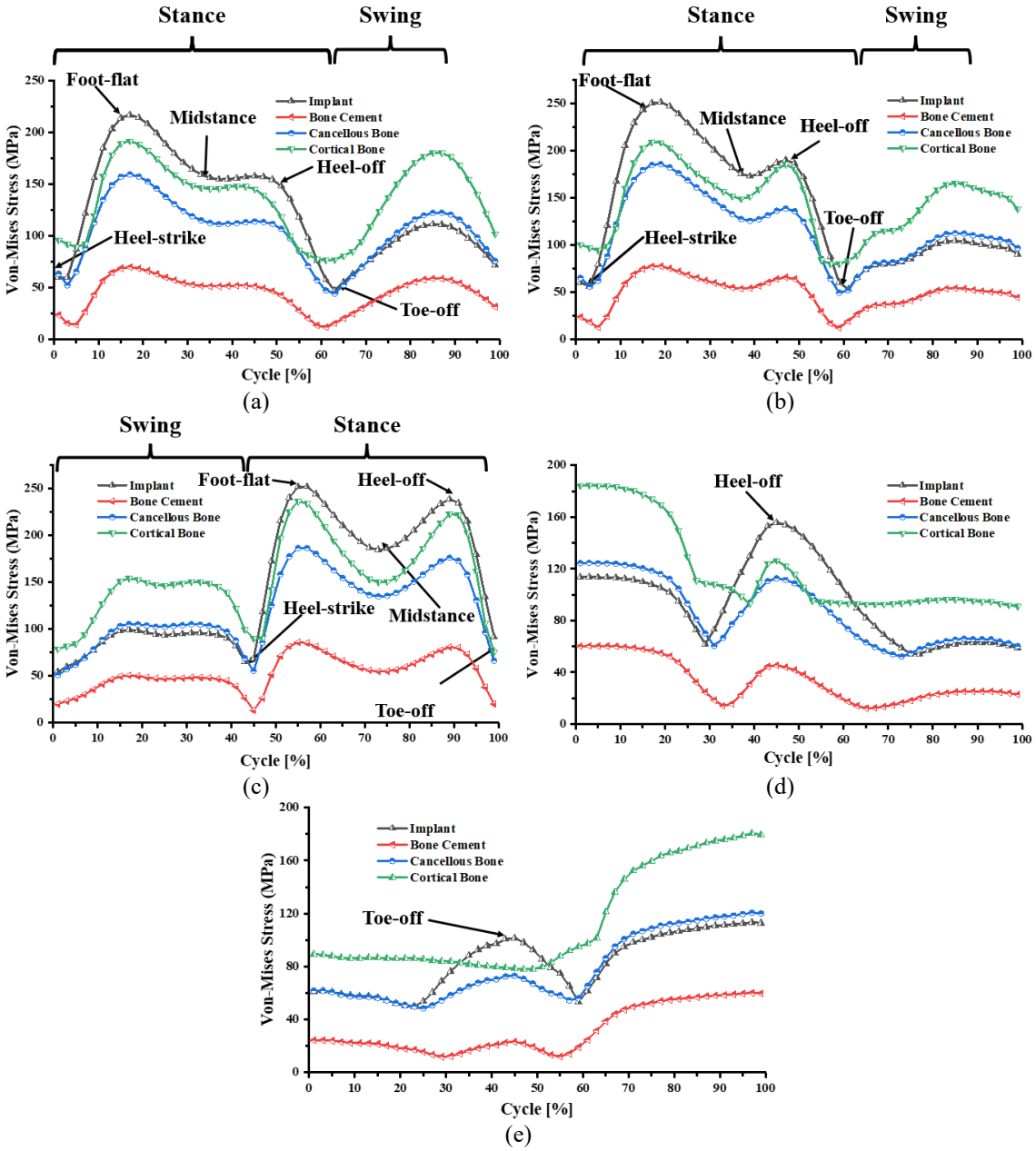

Figure 9. Von Mises stress observed by hip assembly, (a) walking; (b) going up stairs; (c) going down stairs; (d) standing up and (e) sitting down.

Deformation

The application of the dynamic forces and torsional moments leads to deformation in the hip assembly. The maximum deformation observed by the hip assembly at four main instances, i.e., 25, 50, 75 and 100% are shown in Figure 10. It can be seen that the maximum deformation occurs at the proximal side of the bone and continuously reduces toward the distal end. In addition, cortical bone and cancellous bone demonstrate the maximum and minimum deformation, respectively (see Figure 10(b) and 10(e)).

Maximum deformation for different dynamic motions, i.e., walking, going upstairs, going downstairs, standing up and sitting down, are represented in Figures 11(a) to 11(e) respectively. The values of deformation for all assemblies seem approximately similar. However, careful investigation revealed that the implant observed the maximum deformation followed by cortical bone, cancellous bone and lastly by bone cement for each dynamic activity.

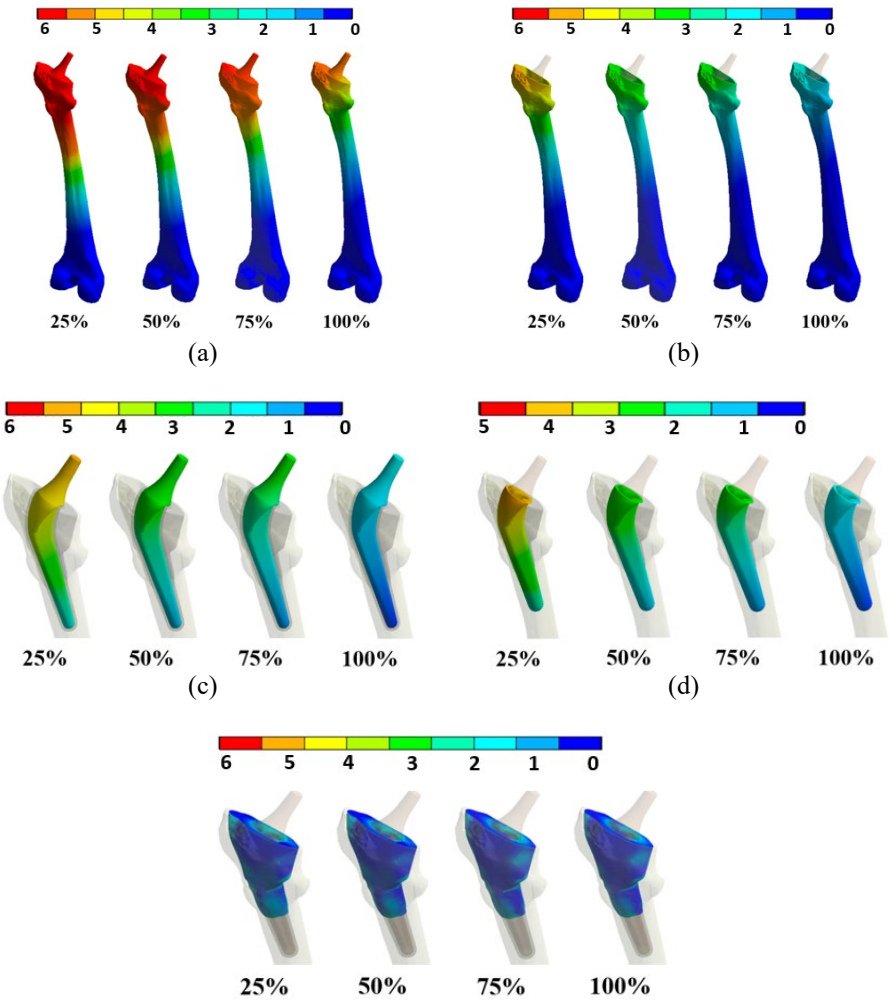

Figure 10. Max. deformation for walking at various percentages of the gait cycle; (a) bone assembly, (b) cortical bone, (c) implant, (d) bone cement and (e) cancellous bone.

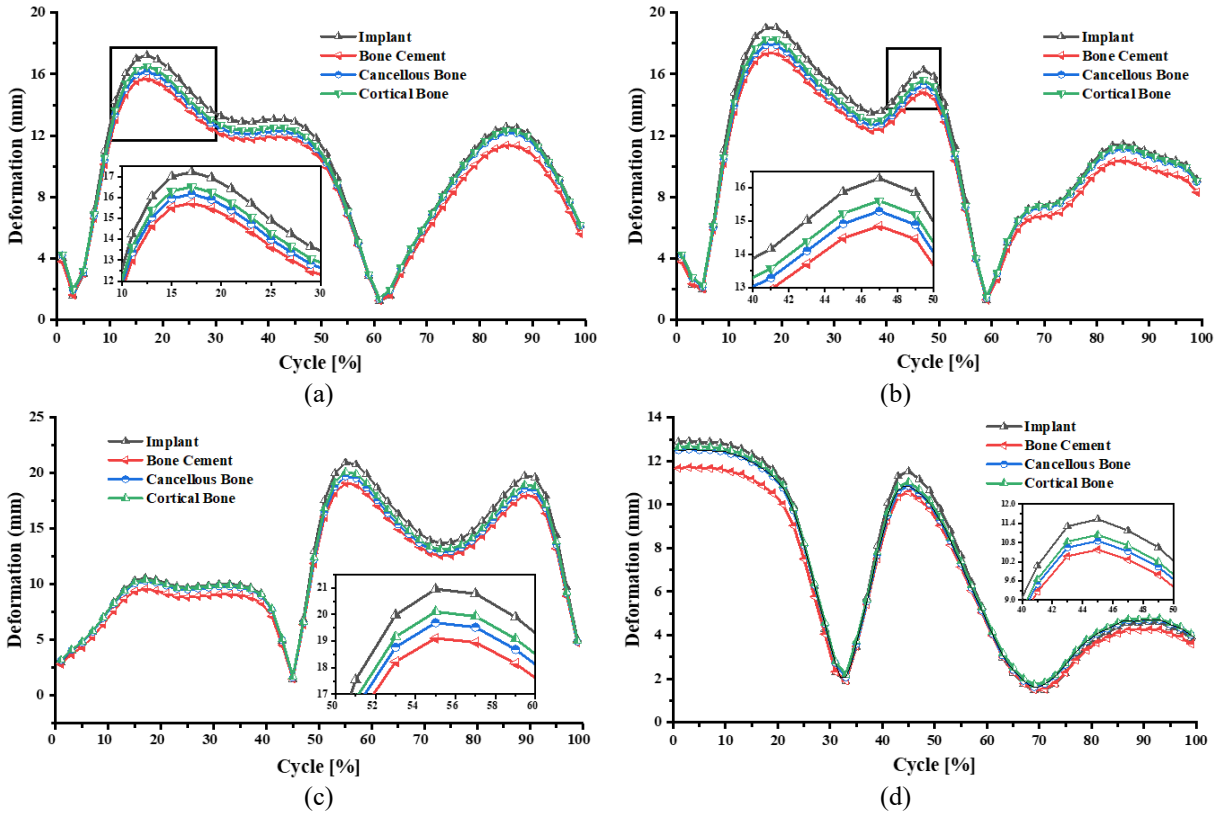

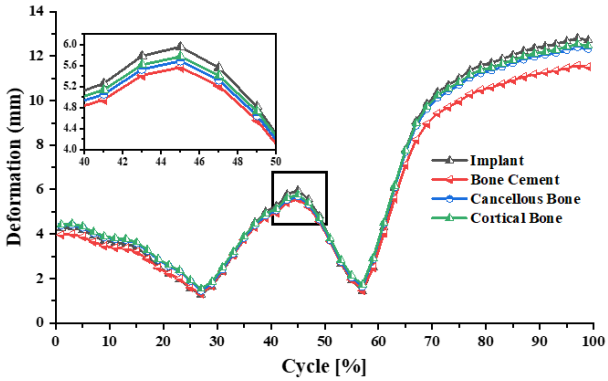

Figure 11. Deformation observed by hip assembly: (a) walking; (b) going up stairs; (c) going down stairs; (d) standing up and (e) sitting down.

Strain

Figure 12(a) to 12(e) presents the strain distribution in the different parts of hip assembly like cortical bone, cancellous bone, bone cement and implant at different gait instances. Similar to deformation distribution, the maximum strain is attained by bone assembly, cortical bone, implant, bone cement and cancellous bone in four instances of 25, 50, 75 and 100% of gait instances respectively. Cancellous bone has shown the maximum, and implant demonstrates the minimum strain. In addition, the lateral side of bone demonstrates the maximum strain, while the proximal end of the implant and cancellous bones also depicts the same (see Figure 12).

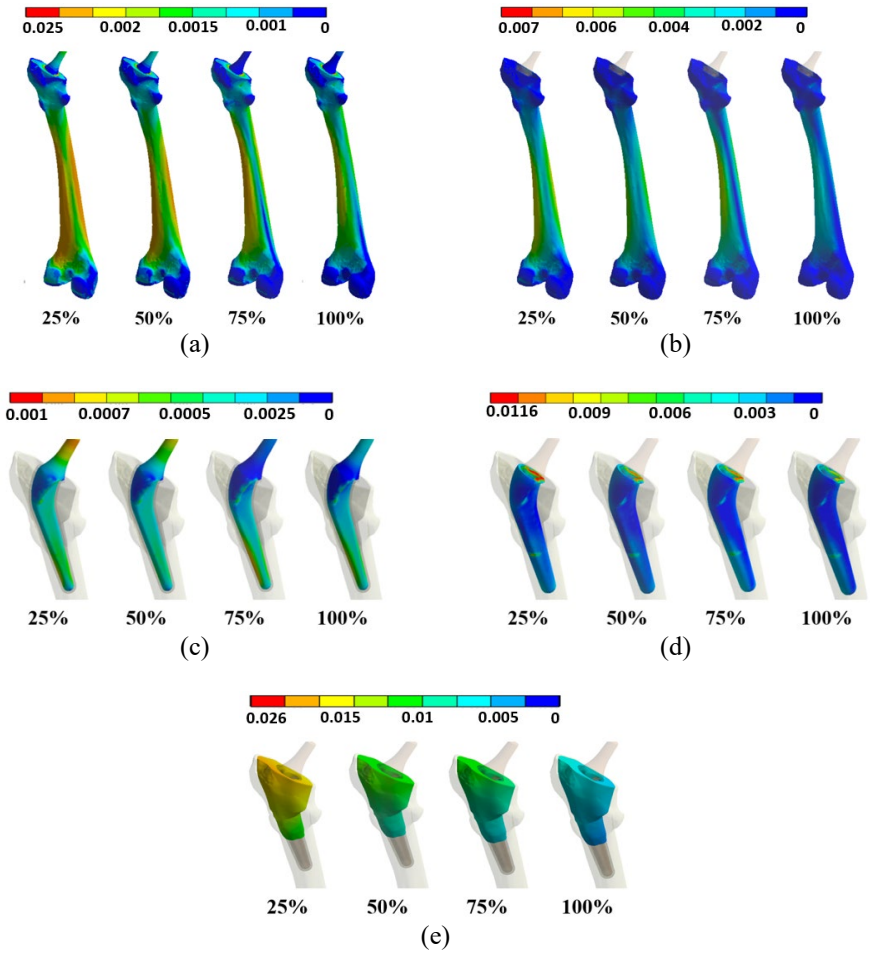

Figure 12. Max. strain for walking at various percentages of the gait cycle; (a) bone assembly, (b) cortical bone, (c) implant, (d) bone cement and (e) cancellous bone.

Figures 13(a) to 13(e) present the maximum strain for different dynamic gait cycles. It can be observed that the cortical bone undergoes the maximum strain and is followed up by bone cement, cancellous bone and lastly, an implant. The peak strain was observed in walking (12-50 %), going upstairs (20-50 %), going downstairs (50-95 %), standing up and sitting down (0-20% and 40-55%), (65-100%) of the gait cycle.

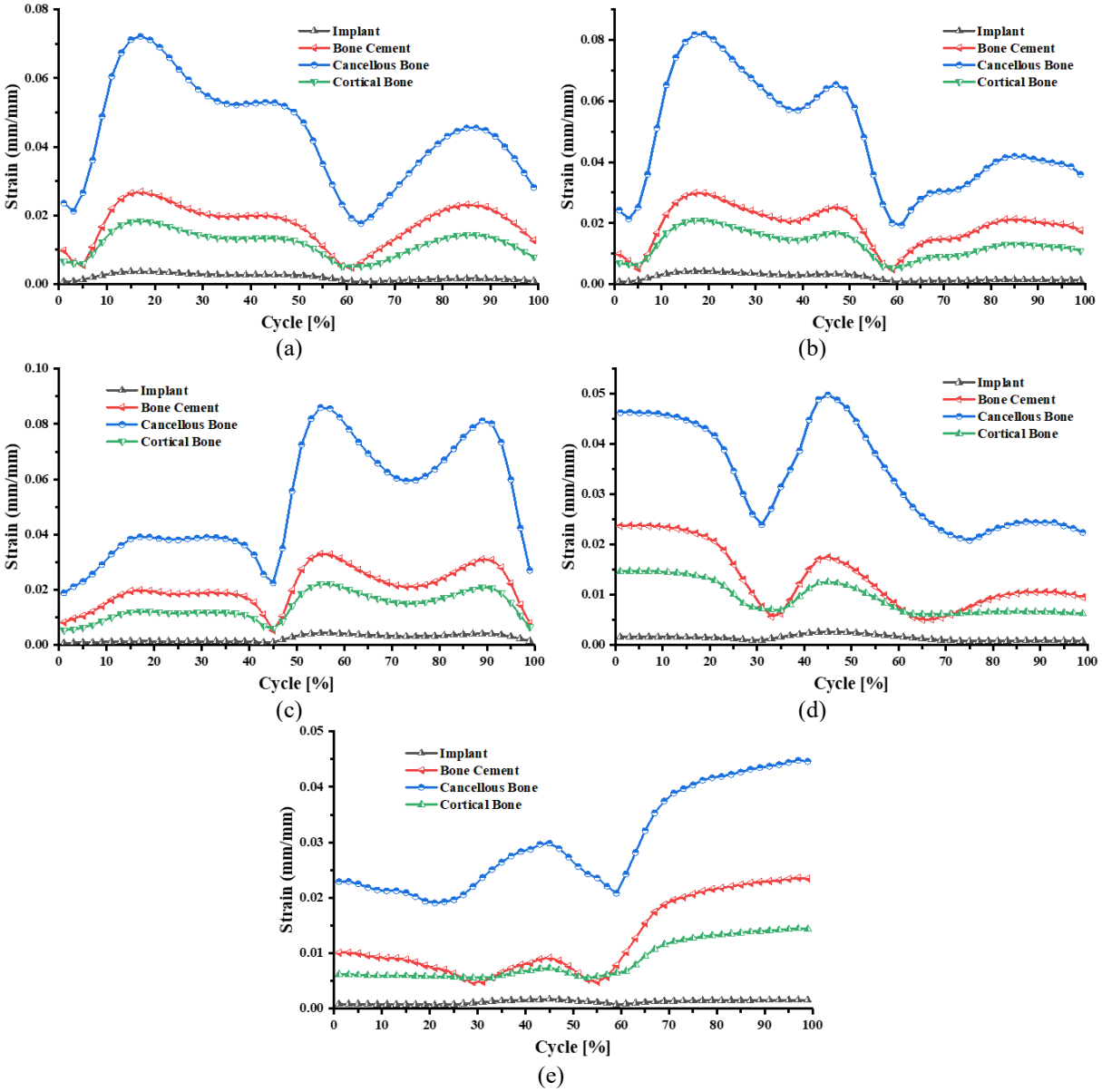

Figure 13. Max. strain observed by hip assembly, (a) walking; (b) going up stairs; (c) going down stairs; (d) standing up and (e) sitting down.

Fatigue Analysis

An implant must satisfy the maximum or infinite fatigue life to minimize the fatigue effect on the bone cement. The fatigue life can only be calculated by experimental testing or fatigue analysis. In the present study, the fatigue life of the prosthesis is calculated with the help of finite analysis code ANSYS. In order to get the fatigue life, the S-N curve is an essential parameter that shows the relation between alternating stress and the number of cycles. The values of S-N curve for Ti-6Al-4V and PMMA bone cement were extracted from Kayabasi et al. [40]. Solderberg, Goodman, Gerber and ASME Elliptic fatigue theories were used to calculate the fatigue life of the prosthesis and are illustrated in Table 4.

Table 4. List of fatigue theories with respected formulae [42].

Fatigue theories	Formulation
Solgerberg	$(\sigma_a/S_e) + (\sigma_m/S_y) = 1/N$
Goodman	$(\sigma_a/S_e) + (\sigma_m/S_{ut}) = 1/N$
Gerber	$(N\sigma_a/S_e) + (N\sigma_m/S_{ut})^2 = 1$
ASME elliptic	$(N\sigma_a/S_e)^2 + (N\sigma_m/S_y)^2 = 1$

In Table 4, N indicates the fatigue life safety factor in cycles, S_e indicates endurance limit, S_{ut} indicates ultimate tensile strength of a material. Mean stress (σ_m) and alternating stress (σ_a) are defined as:

$$\sigma_m = \frac{\sigma_{max} + \sigma_{min}}{2} \quad (1)$$

and,

$$\sigma_a = \frac{\sigma_{max} - \sigma_{min}}{2} \quad (2)$$

Every fatigue simulation follows the standard infinite life criteria of N = 10^9 cycles. The minimum safety factors for Ti-6Al-4V implant under five dynamic motions of walking, going downstairs, going upstairs, standing up and sitting down are tabulated in Table 5.

Table 5. A safety factor of Ti-6Al-4V implant under walking, going downstairs, going upstairs, standing up and sitting down gait activities.

Materials	Safety factor				
	Walking	Going downstairs	Going upstairs	Standing up	Sitting down
Solderberg	7.0224	6.3577	5.5502	8.2064	4.2178
Goodman	7.2611	6.5738	5.7389	8.4854	4.3612
Gerber	8.8722	8.0324	7.0123	10.368	5.3289
ASME Elliptic	9.1947	8.3243	7.2671	10.745	5.5226

Table 5 illustrates that Ti-6Al-4V implant validates a greater safety factor under every dynamic gait motion. Standing up and sitting down demonstrate the maximum and minimum safety factors. The maximum fatigue cycle demonstrated by implant and bone cement is 4.58E+07, and 2.28E+07 respectively.

DISCUSSION

General Findings

The present work is the first one of its kind, which develops a fully functioning FE model of femur hip assembly and predicts their mechanical performance under dynamic constraints. Hip arthroplasty consists of four major parts of metallic implant, PMMA bone cement, cancellus and cortical bones. Neither a single point load applied over the hip joint nor a single movement of a leg represents the appropriate outcome of the analysis. Many of the past studies are focused on linear static (only single point load) [19] and simple dynamic gait analysis [42]. A patient-specific gait data replicates actual anatomical loading constraints. A dynamic torsional moment with dynamic forces is extracted from Bergmann et al. [40], Charnley's implant is fitted into femur bone with an interface layer of bone cement between the implant and bone. Von mises stress for different gait activities is depicted in Figure 14.

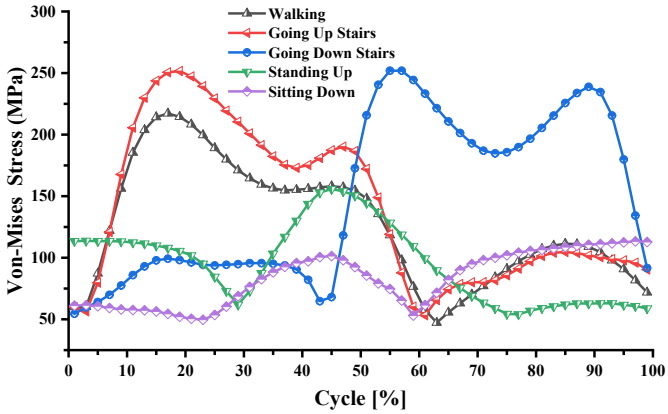

Figure 14. Von Mises stress of hip joint: (a) walking; (b) going up stairs; (c) going down stairs; (d) standing up and (e) sitting down.

Clinical Implantation

Forces and moment replicate actual boundary forces as per the normal anatomic functionality. Implants manufactured by titanium alloys are preferred over cobalt-chromium alloys due to half modulus than Co-Cr alloys. The suitability of an appropriate design for prosthesis plays a very significant role in avoiding loosening and for better anatomical functionality of the human hip joint [43]. Charnley's implant design has been clinically proven and used as the main stem design for the last four to five decades. Implant geometries can easily be modified as per the human anatomy using the simple geometrical technique. Simple proven techniques are compatible with a revision of femur size geometries. PMMA suits as a bone cement having good sticking properties with bone and cement. Ti-6Al-4V implant and PMMA bone cement are within the safety limit under every dynamic activity like walking, standing up and down etc.

Higher stiffness material provides better mechanical stability in the post-operative scenario. However, it may also cause stress shielding, bone loss and implant loosening [44]. While lower stiffness results in increased load transfer to the host femur and leads to bone ingrowth around the implant, minimizing bone loss and improving the stability of implant for the long term [45].

Novel Contribution

Despite some limitations (see Limitation title), there are multiple novel contributions to the present study. This is the only kind of study which replicates the actual force and torque for such a wide range of gait motion of a hip joint and compares mechanical parameters like stress, strain and deformation with the available literature. Prior studies examine the implant assembly only for static analysis under similar boundary conditions [41]. It is a difficult task to apply appropriate constraints while considering all significant forces of the musculoskeletal system. Quantifying change in the loads during dynamic activities is significantly important to check suitability under pre-surgical analysis before being implanted in vivo.

Limitations

Limitations/drawbacks are common for biomechanical investigations. Firstly and foremost limitation, only major muscle force, i.e., abductor muscle force, is considered for the present simulation. The action of all surrounding muscles is limited for the present study. Muscle force demonstrates a significant influence on mechanical parameters like stress, deformation and strain for hip assembly. Secondly, the wear of alloy and cement under repeated cyclic loading conditions has not been investigated in the present study. Third, the effect of femoral head, liner and acetabular cup has not been considered for the present investigation. Fourth, the study is conducted as per the average loading constraints, but it has also been an important factor in simulating assembly under peak dynamic loadings.

Apart from biocompatibility and mechanical properties, some other factors like size and geometrical parameters are some factors that cause some implants to be superior or inferior. The present study is beneficial for future studies to predict the performance of a variety of stem shapes with different materials under every anatomical and muscle force. Every muscle load and torsional moment is to be extracted from the patient-specific models. Such works are beneficial as a future step under the providence of a more clinically relevant scenario.

CONCLUSION

Ti-6Al-4V alloy is the most widely used implant material in the field of biomechanics due to excellent biocompatibility and low chemical inertness. The present work compares the behavior of the prosthesis model for different dynamic activities. The main outcomes of the present investigation are as follows:

i. The cortical bone and bone cement observed the maximum and minimum stress, respectively.
ii. Going upstairs and going downstairs motion demonstrates the maximum stress, while standing up and sitting down demonstrates the minimum.
iii. Implant and bone cement demonstrate maximum and minimum stress simultaneously.
iv. The cortical and cancellous bone observed maximum and minimum deformation respectively.
v. Implant and bone cement demonstrated the maximum and minimum deformation at every gait cycle.
vi. The maximum strain is demonstrated by cancellous bone at the proximal end of the bone.
vii. Cancellous bone and implant demonstrate the maximum and minimum strain simultaneously.
viii. Going downstairs moment leads to higher strain, while standing up and sitting down demonstrate the minimum strain.
ix. The maximum stress, deformation and strain were observed in walking (12-50 %), going upstairs (20-50 %), going downstairs (50-95 %), standing up and sitting down (0-20% and 40-55%), (65-100%) of the gait cycle.
x. Fatigue analysis concluded that the life expectancy of Ti-6Al-4V implant is to be a minimum of 23 years in an active patient.

Analysis of the patient-specific model with multiple gait cycle data demonstrates that the present hip joint model gives us adequate results. This study is endorsed for the patient surgical implantation and also be advantageous for biomedical engineers/doctors/surgeons for further research and to simulate diverse models pre-surgically.

ACKNOWLEDGEMENT

The authors would like to thank Dr. Harsh Singh Airi (MS Orthopedics) for his valuable suggestions regarding the human hip joint, muscle force and gait motion. Furthermore, the author would also like to thank Dr. Kuldeep Yadav (MBBS) of District Hospital Champawat for providing his appreciated information in terms of hip joint modeling for the present research work.

CONFLICT OF INTEREST

The authors declare that they have no known competing financial interests or personal relationships that could have appeared to influence the work reported in this paper.

REFERENCES

[1] S. Savilahti, I. Myllyneva, K.J.J. Pajamäki, and TS Lindholm, "Survival of Lubinus straight (IP) and curved (SP) total hip prostheses in 543 patients after 4–13 years," *Arch. Orthop. Trauma Surg.,* vol. 116, pp. 10–3, 1997 doi: 10.1007/BF00434092.

[2] R.A. Marston, A.G. Cobb, and G. Bentley, "Stanmore compared with Charnley total hip replacement: a prospective study of 413 arthroplasties," *J. Bone Joint Surg. Br. Vol.,* vol. 78, pp.178–84, 1996, doi: 10.1302/0301-620X.78B2.0780178.

[3] L. Neumann, K.G. Freund, and K.H. Sorenson, "Long-term results of Charnley total hip replacement. Review of 92 patients at 15 to 20 years," *J. Bone Joint Surg. Br. Vol*., 1 vol. 76, pp. 245–51, 994,doi: 10.1302/0301-620X.76B2.8113285.

[4] CP Delaunay, and A.I. Kapandji, "Primary total hip arthroplasty with the Karl Zweymüller first-generation cementless prosthesis: A 5-to 9-year retrospective study," *J. Arthroplasty,* vol. 11, pp. 643–52, 1996, doi: 10.1016/S0883-5403(96)80001-5.

[5] T.S. Rubak, S.W. Svendsen, K. Søballe, and P. Frost, "Total hip replacement due to primary osteoarthritis in relation to cumulative occupational exposures and lifestyle factors: a nationwide nested case–control study," *Arthritis Care Res.,* vol. 66, pp. 1496–1505, 2014, doi: 10.1002/acr.22326.

[6] C. Dopico-González, A.M. New, and M. Browne, "Probabilistic finite element analysis of the uncemented hip replacement effect of femur characteristics and implant design geometry," *J. Biomech.,* vol. 43, pp. 512–520, 2010, doi: 10.1016/j.jbiomech.2009.09.039.

[7] E. Ebramzadeh *et al.*, "Long-term radiographic changes in cemented total hip arthroplasty with six designs of femoral components," *Biomaterials,* vol. 24, pp. 3351–3363, 2003, doi: 10.1016/S0142-9612(03)00187-X.

[8] N.G. Sotereanos *et al.*, "Cementless femoral components should be made from cobalt chrome," *Clin. Orthop. Relat. Res.,* vol 313,pp. 146–153, 1995,.

[9] B.M. Wroblewski, and P.D. Siney, "Charnley low-friction arthroplasty of the hip. Long-term results," *Clin. Orthop. Relat. Res.* vol. 292, pp. 191–201, 1993,.

[10] R.A. Ibrahim, "Friction-induced vibration, chatter, squeal, and chaos—part I," *Mechanics of Contact and Friction,* vol. 47, pp. 209–226, 1994, doi: 10.1115/1.3111079.

[11] CIHI. Canadian Institute for Health Information, Hip and knee replacements in Canada (Online) Available: https://www.cihi.ca/en/hip-and-knee-replacements-in-canada-cjrr-annual-report [Accessed May 7, 2021].

[12] G. Garellick, J. Kärrholm, C. Rogmark, and P. Herberts, "Swedish hip arthroplasty register," Annual Report 2009; Department of Orthopaedics, Sahlgrenska University Hospital, Annual Report 2009; Sweden, 2009.

[13] K.J. Bozic *et al.*, "The epidemiology of revision total hip arthroplasty in the United States," *J. Bone Joint Surg.*, vol. 91, pp. 128–133, 2009, doi: 10.2106/JBJS.H.00155.

[14] T.P. Harrigan, and W.H. Harris, "A three-dimensional non-linear finite element study of the effect of cement-prosthesis debonding in cemented femoral total hip components," *J. Biomech.,* vol. 24, pp. 1047–1058, 1991, doi: 10.1016/0021-9290(91)90021-E.

[15] RJ van Arkel, S. Ghouse, P.E. Milner, and J.R.T. Jeffers, "Additive manufactured push-fit implant fixation with screw-strength pull out," *J. Orthop. Res.,* vol. 36, pp. 1508–1518, 2018, doi: 10.1002/jor.23771.

[16] U. Hossain, S. Ghouse, K. Nai, and J.R. Jeffers, "Controlling and testing anisotropy in additively manufactured stochastic structures," *Addit. Manuf.,* vol. 39, 101849, 2021, doi: 10.1016/j.addma.2021.101849.

[17] M. Ikeda, S-Y. Komatsu, I. Sowa, and M. Niinomi, "Aging behavior of the Ti-29Nb-13Ta-4.6 Zr new beta alloy for medical implants," *Metall. Mater. Trans. A:,* vol. 33, pp. 487–493, 2002, doi: 10.1007/s11661-002-0110-9.

[18] M. Geetha, A.K. Singh, R. Asokamani, and A.K. Gogia, "Ti based biomaterials, the ultimate choice for orthopaedic implants–a review," *Prog. Mater. Sci.,* vol. 54, pp. 397–425, 2009, doi: 10.1016/j.pmatsci.2008.06.004.

[19] H. Bougherara *et al.*, "A preliminary biomechanical study of a novel carbon–fibre hip implant versus standard metallic hip implants," *Med. Eng. Phys.,* vol. 33, pp. 121–128, 2011, doi: 10.1016/j.medengphy.2010.09.011.

[20] J.A. Simões, and A.T. Marques, "Design of a composite hip femoral prosthesis," *Mater. Des.,* vol 26, pp. 391–401, 2005, doi: 10.1016/j.matdes.2004.07.024.

[21] M. Niinomi, "Recent research and development in titanium alloys for biomedical applications and healthcare goods," *Sci. Technol. Adv. Mate.,* vol. 4, pp. 445, 2003, doi: 10.1016/j.stam.2003.09.002.

[22] P. Laheurte, A. Eberhardt, and M-J. Philippe, "Influence of the microstructure on the pseudoelasticity of a metastable beta titanium alloy," *Mater. Sci. Eng.: A*, vol. 396, pp. 223–230, 2005, doi: 10.1016/j.msea.2005.01.022.

[23] N. Goetzen, F. Lampe, R. Nassut, and M.M. Morlock, "Load-shift—numerical evaluation of a new design philosophy for uncemented hip prostheses," *J. Biomech.,* vol. 38, pp. 595–604, 2005, doi: 10.1016/j.jbiomech.2004.01.023.

[24] S.T. Gross, and E.W. Abel, "A finite element analysis of hollow stemmed hip prostheses as a means of reducing stress shielding of the femur," *J. Biomech.,* vol. 34, pp. 995–1003, 2001, doi: 10.1016/S0021-9290(01)00072-0.

[25] HS Hedia, D.C. Barton, J. Fisher, and T.T. Elmidany, "A method for shape optimization of a hip prosthesis to maximize the fatigue life of the cement," *Med. Eng. Phys.,* vol. 18, pp. 647–654, 1996, doi: 10.1016/S1350-4533(96)00025-2.

[26] H.F. El'Sheikh, B.J. MacDonald, and M.S.J. Hashmi, "Finite element simulation of the hip joint during stumbling: a comparison between static and dynamic loading," *J. Mater. Process. Technol.,* vol. 143, pp. 249–255, 2003, doi: 10.1016/S0924-0136(03)00352-2.

[27] T. Joshi, O. Parkash, and G. Krishan, "Numerical investigation of slurry pressure drop at different pipe roughness in a straight pipe using CFD," *Arab. J. Sci. Eng.,* vol. 57, pp. 1-24, 2022, doi: 10.1007/s13369-022-06583-1.

[28] T. Joshi, O. Parkash, and G. Krishan, "CFD modeling for slurry flow through a horizontal pipe bend at different Prandtl number," *Int. J. Hydrog. Energy,* vol. 47, pp. 23731–23750, 2022, doi: 10.1016/j.ijhydene.2022.05.201.

[29] T. Joshi, R. Sharma, O. Parkash, and A. Gupta, "Design and analysis of metal-to-metal contact bolted flange joint using FEA tool," In: P. Joshi, S.S. Gupta, A.K. Shukla, S.S. Gautam, editors. *Advances in Engineering Design*, Singapore: Springer; 2021, pp. 315–25, doi: 10.1007/978-981-33-4684-0_32.

[30] T. Joshi, and S. Kant, "A Review on Finite Element Analysis of Leaf Spring for Composite Material," *Int. J. Innov. Sci. Res. Technol.,* vol. 3, pp. 399–409, 2018.

[31] T. Joshi, R. Sharma, V. Kumar Mittal, and V. Gupta, "Comparative investigation and analysis of hip prosthesis for different bio-compatible alloys," *Mater. Today: Proc.,* vol. 43, pp. 105–111, 2021, doi: 10.1016/j.matpr.2020.11.222.

[32] T. Joshi, and G. Gupta, "Effect of dynamic loading on hip implant using finite element method," *Mater. Today: Proc.,* vol. 43, pp. 105-111, 2021, doi: 10.1016/j.matpr.2020.11.378.

[33] T. Joshi, R. Sharma, V.K. Mittal, V. Gupta, and G. Krishan, "Dynamic Analysis of Hip Prosthesis Using Different Biocompatible Alloys," *ASME Open J. Eng.,* vol. 1, p. 011001, 2022,doi: 10.1115/1.4053417.

[34] S.J. Incavo, BD. Beynnon, and K.M. Coughlin, "Total hip arthroplasty with the secur-fit and secur-fit plus femoral stem design: a brief follow-up report at 5 to 10 years," *J. Arthroplasty,* vol. 23, pp. 670–676, 2008, doi: 10.1016/j.arth.2007.05.044.

[35] Y.K. Kang *et al.*, "Three dimensional shape reconstruction and finite element analysis of femur before and after the cementless type of total hip replacement," *J. Biomed. Eng.,* vol. 15, pp. 497–504, 1993, doi: 10.1016/0141-5425(93)90065-7.
[36] A.D. Speirs *et al.*, "Three-dimensional measurement of cemented femoral stem stability: an in vitro cadaver study," *Clin. Biomech.* vol. 15, pp. 248–255, 2000, doi: 10.1016/S0268-0033(99)00079-0.
[37] A.D. Speirs *et al.*, "Three-dimensional measurement of cemented femoral stem stability: an in vitro cadaver study," *Clin. Biomech.* vol.15, pp. 248–255, 2000, https://doi.org/10.1016/S0268-0033(99)00079-0
[38] E. Peltola *et al.*, "Materials used for hip and knee implants. Wear of orthopaedic implants and artificial joints," vol. 1, pp. 178–218, 2013. https://doi.org/10.1533/9780857096128.1.178.
[39] A.Z. Senalp, O. Kayabasi, and H. Kurtaran, "Static, dynamic and fatigue behavior of newly designed stem shapes for hip prosthesis using finite element analysis," *Mater. Des.,* vol. 28, pp. 1577–1583, 2007, doi: 10.1016/j.matdes.2006.02.015.
[40] G. Bergmann *et al.*, "Realistic loads for testing hip implants," *Bio-Med. Mater. Eng.* vol. 20, pp. 65–75, 2010, doi: 10.3233/BME-2010-0616.
[41] A.T. Şensoy, M. Çolak, I. Kaymaz, and F. Findik, "Optimal material selection for total hip implant: A finite element case study," *Arab. J. Sci. Eng.,* vol. 44, pp. 10293–10301, 2019, doi: 10.1007/s13369-019-04088-y.
[42] O. Kayabasi, and B. Ekici, "The effects of static, dynamic and fatigue behavior on three-dimensional shape optimization of hip prosthesis by finite element method," *Mater. Des.,* vol. 28, pp. 2269–2277, 2007, doi: 10.1016/j.matdes.2006.08.012.
[43] K. Chalernpon, P. Aroonjarattham, and K. Aroonjarattham, "Static and dynamic load on hip contact of hip prosthesis and Thai femoral bones," *Int. J. Mech. Mechatron. Eng.,* vol. 9, pp. 251–255, 2015, doi: 10.5281/zenodo.1099670.
[44] D.R. Sumner *et al.*, "Functional adaptation and ingrowth of bone vary as a function of hip implant stiffness," *J. Biomech.,* vol. 31, pp. 909–917, 1998, doi: 10.1016/S0021-9290(98)00096-7.
[45] B. Van Rietbergen *et al.*, "The mechanism of bone remodeling and resorption around press-fitted THA stems," *J. Biomech.,* vol. 26, pp. 369–382, 1993, doi: 10.1016/0021-9290(93)90001-U.